



Contents lists available at ScienceDirect

## Corrosion Science

journal homepage: [www.elsevier.com/locate/corsci](http://www.elsevier.com/locate/corsci)

## Surface recrystallization and its effect on oxidation of superalloy C263

Naicheng Sheng<sup>a,\*</sup>, Katharina Horke<sup>b</sup>, Andreas Meyer<sup>a</sup>, Martin R. Gotterbarm<sup>a</sup>, Ralf Rettig<sup>c</sup>, Robert F. Singer<sup>a,c</sup><sup>a</sup> Joint Institute of Advanced Materials and Processes (ZMP), Friedrich-Alexander University of Erlangen-Nuremberg (FAU), Dr.-Mack-Str. 81, D-90762 Fuerth, Germany<sup>b</sup> Rolls-Royce Deutschland Ltd. & Co. KG, Eschenweg 11, Dahlewitz, 15827 Blankenfelde-Mahlow, Germany<sup>c</sup> ThermoCalc Software AB, Norra Stationsgatan 93, SE-113 64 Stockholm, Sweden

## ARTICLE INFO

## Keywords:

- A. Superalloys
- B. SEM
- B. EPMA
- B. XRD
- C. Oxidation

## ABSTRACT

Ni-base superalloy C263 has been oxidized from 700 °C to 1100 °C in artificial dry air. A continuous Cr rich (Cr, Ti)<sub>2</sub>O<sub>3</sub> layer is formed during oxidation, while the oxidation kinetics deviated from the parabolic kinetics. The oxidation microstructures were different in as-machined and polished samples. Recrystallization below the oxide layer occurred in as-machined samples together with severe internal degradation (internal oxidation and nitridation). Grain boundaries provide paths for fast diffusion of O and N into the substrate and outward diffusion of Ti and Cr. Surface deformation and recrystallization exhibit detrimental effects on the oxidation behavior of C263.

## 1. Introduction

The harsh environment in advanced turbine engines has led to the application of superalloy parts in hot sections [1]. Besides the requirement of adequate mechanical properties (creep, fatigue etc. [2]), oxidation properties are also important [3,4]. Cr and Al are usually added to form protective Cr<sub>2</sub>O<sub>3</sub> or Al<sub>2</sub>O<sub>3</sub> layers to improve the oxidation resistance of superalloys [5–7]. Although Al<sub>2</sub>O<sub>3</sub> layers show a smaller growth rate at high temperatures than Cr<sub>2</sub>O<sub>3</sub> layers [8], they are more brittle and the adherence between the Al<sub>2</sub>O<sub>3</sub> layer and substrate is poorer compared to Cr<sub>2</sub>O<sub>3</sub> layers [9–11]. Additionally, Al<sub>2</sub>O<sub>3</sub> is less protective under sulfidation conditions [12]. A further consideration is as follows: Al, when added in sufficient quantity, leads to  $\gamma'$ -formation and high strength, making rolling and forging much more difficult [13]. Since high strength is not always required, many wrought superalloys are designed to form a Cr<sub>2</sub>O<sub>3</sub> layer [14].

During oxidation, the substrate region close to the Cr<sub>2</sub>O<sub>3</sub> layer will be depleted in Cr and degraded by the penetration of oxygen and nitrogen (internal oxidation or nitridation) [15–17]. As a result, the mechanical properties are decreased. Crack propagation may be accelerated by the internal degradation process [18–20]. Oxides such as Al<sub>2</sub>O<sub>3</sub>, and nitrides like TiN, AlN and even CrN phases could form during the internal degradation process [21–23]. Once these oxides/nitrides are formed, the volume change in the matrix will introduce high stresses in the oxide layer [24] and the layer may even be damaged. Once the chromia layer is cracked, then faster penetration of O/

N will further accelerate the internal oxidation and nitridation of the alloys [25,26]. The internal oxides preferably grow along the grain boundaries which provide easy propagation paths for cracks during mechanical loading [26,27]. The formation of a Cr<sub>2</sub>O<sub>3</sub> layer can be affected by surface finish, such as sand blasting, rolling and grinding [28,29]. Research showed that surface deformation could improve the formation of a surface oxide layer [29,30]. However, the exact effects of surface finish on the internal degradation (Cr depletion, internal oxidation or nitridation) are still unclear.

The material investigated in the present paper, Nimonic C263 (C263 for short), is a solution and age-hardenable Ni-base superalloy containing 20 wt.% Cr, 2.0 wt.% Ti and 0.45 wt.% Al [31]. According to the investigations on similar Ni-Cr-Al alloys [32], a chromia scale will form during the oxidation. Little is known about the oxidation behavior of this alloy. Previous research usually focused on its machining, microstructures and deformation mechanism [33–35]. In the present work, the oxidation behavior of C263 superalloy after machining was investigated from 700 °C to 1100 °C in artificial dry air.

## 2. Experimental conditions

C263 superalloy plates were received from Rolls-Royce Deutschland Ltd & Co KG. The materials were first rolled, solution heat treated at 1150 °C followed by air cooling and then finally aged at 800 °C for 8 h. The composition of superalloy C263 measured via spark spectrometry (SpectroMaXx arc spark OES metal analyzer, SPECTRO Analytical

\* Corresponding author.

E-mail address: [naicheng.sheng@fau.de](mailto:naicheng.sheng@fau.de) (N. Sheng).<http://dx.doi.org/10.1016/j.corsci.2017.09.020>Received 22 April 2017; Received in revised form 30 August 2017; Accepted 15 September 2017  
0010-938X/© 2017 Elsevier Ltd. All rights reserved.

**Table 1**  
Composition of C263 superalloy measured by spark spectrometry.

	Ni	Co	Cr	Mo	Ti	Al	Mn	Fe	C	B	Si	Cu	S
wt.%	Bal.	19.45	20.50	5.95	2.22	0.48	0.24	0.36	0.08	0.002	0.092	0.012	0.004
at.%	Bal.	19.39	18.04	9.66	1.80	0.22	0.22	0.34	0.016	0.0004	0.044	0.013	0.002

Instruments GmbH, Germany) is shown in Table 1. Specimens for oxidation tests were machined from the as-received plates to dimensions of 7 mm × 40 mm × 2 mm. After that, the surfaces of the specimens were milled and ground with SiC grit < #1000 to obtain surface roughness  $R_a < 0.3 \mu\text{m}$  according to MSRR9968. One specimen was afterwards mechanically polished to study the effect of machining on the oxidation microstructure. The specimen was first polished with SiC grinding paper (#80–#4000 grit, Struers GmbH, Germany) to remove the strains introduced from machining, and then they were final polished using standard colloidal silica suspension (OP-U, Struers GmbH, Germany) on a semi-automatic polishing machine (Tegramin, Struers GmbH, Germany). Before oxidation, specimens were cleaned in ethanol using an ultrasonic bath for 5 min to remove surface contaminations. The substrate microstructures of as received specimen and oxidized specimens at different temperatures were prepared through polishing (first grinding with #80–#4000 grit, then final polishing using OP-U and cleaning with demineralized water) and etching with V2A etchant (100 ml demineralized water, 100 ml 32% HCl, 15 ml 65% HNO<sub>3</sub>) for 15 s. Substrate microstructures were checked using scanning electron microscopy (SEM, Quanta 450, FEI, USA).

Oxidation tests were performed in the furnace with 20% O<sub>2</sub>/80% N<sub>2</sub> artificial dry air (gas flow rate 15 L/h) at 700 °C, 800 °C and 900 °C for up to 300 h. Three specimens were put in the furnace (Nabertherm LE1, Carbolite Gero GmbH & Co. KG, Germany) in each condition and the oxidation test was stopped at the pre-designated time for weighing. The weight of the specimens was recorded using an analytical balance with an accuracy of  $1 \times 10^{-5}$  g. At 60 h, 200 h and 300 h, one of the specimens was removed, and naturally cooled in air (20 °C). Supplemental oxidation experiments of C263 at 800 °C for 30 h/120 h/250 h/400 h were also carried out in order to get a better understanding of the evolution of the internal degradation (ID) process. Oxidation at 1000 °C and 1100 °C for 60 h were also conducted using a thermo-gravimetric analyzer (Setaram Evolution 1650, France) to have a better understanding of the oxidation process early on.

After oxidation, surface morphologies were examined using a light microscope (Axio Imager.M1m, ZEISS, Germany) and SEM (Quanta 450, FEI, USA) and the compositions of oxides were analyzed through energy dispersive X-Ray spectroscopy (EDS). The depths of the internal oxidation and recrystallization were measured using the ImageJ software [36]. The areas of the internal oxidation and surface

recrystallization were calculated first, and divided by the length of the image to obtain the average depth. At least three SEM images of different areas were used for statistic. X-ray diffraction (XRD) measurements were performed on the fresh surfaces of machined and polished specimens oxidized at 800 °C for 60 h. For in-depth analysis of the surface region several EBSD measurements were made. Specimens for normal EBSD analysis were cut and polished metallographically (first grinding with #80–#4000 grit SiC grinding paper, then final polishing using OP-U and cleaning with demineralized water). The specimens for High Resolution-EBSD (HR-EBSD) analysis were additionally ion beam polished with a Leica EM TIC 3X Ion milling System (Leica Microsystems GmbH, Germany) after metallographical preparation. All EBSD measurements were conducted on a FEI Helios NanoLab 600i FIB Workstation equipped with an Oxford Instruments NordlysNano EBSD detector. The patterns were recorded at an acceleration voltage of 25 kV using the Oxford Instruments AZtechHKL software. The EBSD data analysis was done with the Oxford Instruments HKL CHANNEL5 software. For the HR-EBSD measurements the step size was set to 0.1  $\mu\text{m}$ , the patterns were recorded with a resolution of 1344 × 1024 Pixels and data analysis was done with the commercial software CrossCourt4 (CC4) from BLG Vantage Software Inc. CC4 performs cross-correlation analysis of the collected EBSPs to detect residual elastic and plastic strains. The method is described elsewhere in detail [37–40]. Mapping of the element distribution in the oxidation areas of machined and polished specimens was performed using electron probe micro analysis (EPMA) (JXA-8100, JEOL, Japan).

### 3. Results

#### 3.1. Bulk substrate morphologies

The microstructures of as-machined alloy have been examined and are shown in Fig. 1a. The substrate material exhibits a rather wide grain size distribution. The grains are twinned, indicating grain growth during annealing. No obvious precipitates are observed along the grain boundaries (small figure at up left corner in Fig. 1a), but stringers of small size precipitates (Fig. 2) are distributed parallel to the rolling direction. The substrate microstructures changed after oxidation at 700 °C, 800 °C and 900 °C for 300 h. As observed in Fig. 1b–d, very fine precipitates formed along the grain boundaries at 700 °C, 800 °C and

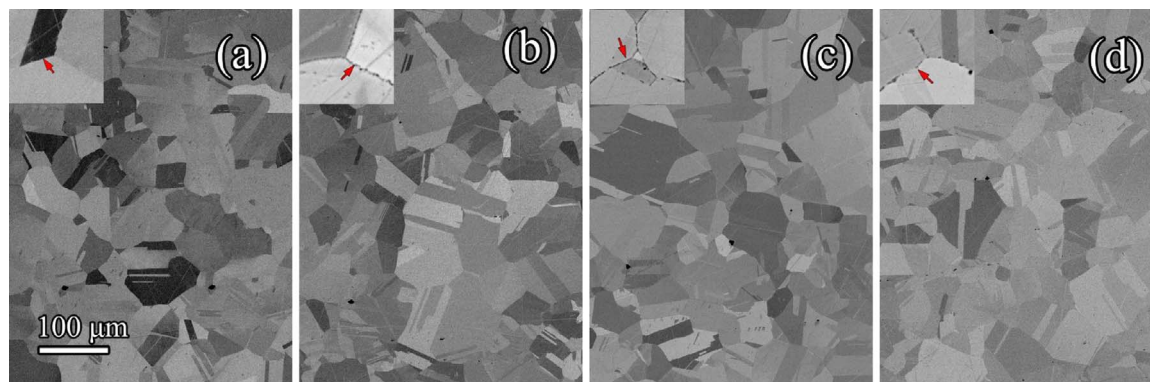


**Fig. 1.** (a) Substrate microstructures of as-machined and (b) to (d) substrate microstructures of specimens oxidized at 700 °C, 800 °C and 900 °C for 300 h, respectively. Grain boundary morphologies for each condition are illustrated by red arrows in the small picture in the upper left corner. (Etched with V2A etchant, SEM-BSE mode). (For interpretation of the references to colour in this figure legend, the reader is referred to the web version of this article.)

Download English Version:

<https://daneshyari.com/en/article/7894297>

Download Persian Version:

<https://daneshyari.com/article/7894297>

[Daneshyari.com](https://daneshyari.com)